The three-dimensional molecular structure of the desmosomal plaque

Ashraf Al-Amoudi[a,1], Daniel Castaño-Diez[a], Damien P. Devos[a,2], Robert B. Russell[a,b], Graham T. Johnson[c], and Achilleas S. Frangakis[a,d,3]

[a]Structural and Computational Biology Unit, European Molecular Biology Laboratory, 69117 Heidelberg, Germany; [b]Cell Networks, University of Heidelberg, 69120 Heidelberg, Germany; [c]The Scripps Research Institute, La Jolla, CA 92037; and [d]Frankfurt Institute for Molecular Life Science and Institute of Biophysics, Goethe University Frankfurt, 60438 Frankfurt, Germany

Edited by Barry H. Honig, Columbia University/Howard Hughes Medical Institute, New York, NY, and approved March 10, 2011 (received for review December 27, 2010)

The cytoplasmic surface of intercellular junctions is a complex network of molecular interactions that link the extracellular region of the desmosomal cadherins with the cytoskeletal intermediate filaments. Although 3D structures of the major plaque components are known, the overall architecture remains unknown. We used cryoelectron tomography of vitreous sections from human epidermis to record 3D images of desmosomes in vivo and in situ at molecular resolution. Our results show that the architecture of the cytoplasmic surface of the desmosome is a 2D interconnected quasiperiodic lattice, with a similar spatial organization to the extracellular side. Subtomogram averaging of the plaque region reveals two distinct layers of the desmosomal plaque: a low-density layer closer to the membrane and a high-density layer further away from the membrane. When combined with a heuristic, allowing simultaneous constrained fitting of the high-resolution structures of the major plaque proteins (desmoplakin, plakophilin, and plakoglobin), it reveals their mutual molecular interactions and explains their stoichiometry. The arrangement suggests that alternate plakoglobin–desmoplakin complexes create a template on which desmosomal cadherins cluster before they stabilize extracellularly by binding at their N-terminal tips. Plakophilins are added as a molecular reinforcement to fill the gap between the formed plaque complexes and the plasma membrane.

vitreous sectioning | image processing | genetic algorithms | multi-protein fitting

Cell junctions are widely distributed in animal tissues and are most abundant in tissues that are subjected to considerable mechanical stress, such as heart, epidermis, and muscle. These junctions are composed of two main classes of proteins: transmembrane adhesion proteins with an extracellular domain that interacts with either the ECM (e.g., focal adhesion and hemidesmosome) or the extracellular domains of specific transmembrane adhesion proteins from the juxtaposed cell (e.g., adherens junctions and desmosomes); and a cytoplasmic tail that binds to one or more intracellular anchor proteins. These form a distinct plaque on the cytoplasmic face of the plasma membrane and connect the junctional complexes to actin filaments or intermediate filaments (IFs). When they have been assembled, these junctions play essential roles in tissue morphogenesis and maintenance; plaque disruption is a hallmark of many blistering and cancer diseases (1, 2). Biochemical and mutagenesis studies have revealed many interactions between the plaque components and their connections to the extracellular space (3–8). However, the organization and interactions of the constituent proteins in the context of the assembled junctions remain poorly understood. For example, whether or how actin filaments bind in situ to the adherens junctions and how the anchoring proteins in hemidesmosome plaque connect integrin to the IFs is still unclear.

In the current study, we present the 3D cytoplasmic surface of the desmosome—the desmosomal plaque—from human epidermis. The desmosomal plaque consists of two electron-dense regions: the outer dense plaque (ODP) is located closer to the plasma membrane, and the inner dense plaque (IDP) is further away from the membrane. The ODP consists of two major armadillo family members, plakoglobin and plakophilin, which mediate the binding of cadherin cytoplasmic tails to the N terminus of desmoplakin, which itself constitutes most of the IDP and tethers to the IFs (1, 2). Despite many efforts, the molecular architecture of the desmosomal plaque components remains unknown because of its large size and complex composition. The challenge is both technical and functional: first, although most of our phenotypic knowledge of the desmosome morphology has been derived from EM studies of thin sections, the use of heavy-metal staining has resulted in the plaque appearing extremely electron-dense without significant distinguishable features (9–11). Hence, the arrangement of the macromolecules could not be resolved. Second, the molecular organization and the stoichiometry of the plaque in situ, which is essential for maintaining and regulating the adhesion of desmosomal cadherins in the extracellular domain and the cytoplasmic interaction with IFs, remain unknown.

Here we use cryoelectron tomography (cryo-ET) of vitreous sections from human desmosomes to visualize the molecular architecture of the plaque. Vitreous cryosectioning has been the "gold standard" of EM preparation methods, which—in contrast to conventional EM preparation methods—does not involve any heavy-metal staining, and does not cause any aggregation. Hence, it provides high-resolution images of ultrastructure at as close to native conditions as possible. However, vitreous cryosectioning in combination with cryo-ET is challenging, mainly because of cutting-induced deformations. Cryosections are usually not flat and have a number of cutting artifacts, including knife marks, crevasses, and cutting-induced compression (12). Most of these problems have been circumvented. Knife marks do not influence the subsequent image processing, and crevasses can be prevented at favorable cutting settings (13). The cutting-induced compression is an inhomogeneous volumetric deformation and thus cannot be corrected in the tomographic reconstructions. A recent

Author contributions: A.A.-A. and A.S.F. designed research; A.A.-A. and A.S.F. performed research; D.P.D., R.B.R., and G.T.J. contributed new reagents/analytic tools; A.S.F. and D.C.-D. analyzed data; and A.A.-A. and A.S.F. wrote the paper.

The authors declare no conflict of interest.

This article is a PNAS Direct Submission.

Freely available online through the PNAS open access option.

Data deposition: The EM density map reported in this paper has been deposited in the EBI Macromolecular Structure Database (accession no. EMD-1374).

[1]Present address: Deutsches Zentrum für Neurodegenerative Erkrankungen, 53175 Bonn, Germany.

[2]Present address: Center for Cellular Imaging and Nanoanalytics (C-CINA), Biozentrum, University of Basel, CH-4056 Basel, Switzerland.

[3]To whom correspondence should be addressed. E-mail: achilleas.frangakis@biophysik.org.

This article contains supporting information online at www.pnas.org/lookup/suppl/doi:10.1073/pnas.1019469108/-/DCSupplemental.

report has shown that compression has an effect mainly at cellular level and has no effect on macromolecular complexes such as ribosomes (14). In addition to these problems, sections are usually not flat and thus are poorly attached to the support film. This is has been resolved adequately with the application of electrostatic charging (15). In combination with 3D subtomogram averaging, cryo-ET of vitreous sections is therefore currently the only way to quantitatively analyze electron tomographic data from eukaryotic cells at arbitrary regions and produce molecular 3D EM density maps. It thus has the potential for analyzing the whole genre of these intercellular junctions. The 3D average map of desmosomes showed a periodic arrangement of the plaque, which closely resembles the molecular organization of the desmosomal cadherins in the extracellular space previously revealed by cryo-ET of vitreous sections (16). We show that the plaque consists of two distinct electron-dense regions separated by an electron-lucent region: a low-density region closer to the membrane and a high-density region further away from the membrane. Fitting of the available X-ray structures of the plaque components into the EM density map by integrating information from immuno-EM data, biochemical methods, and mutagenesis methods leads us to propose a likely configuration of the interacting molecules within the plaque.

Results and Discussion

Cryo-ET Reveals Two Distinct Layers. We first analyzed the general phenotype of the desmosomal region in 2D projection images of vitreous sections from human skin (Fig. 1*A*) and computational slices from the 3D reconstruction (Fig. 1*B*). The extracellular domains of the desmosomal cadherins appear as electron-dense, curved protrusions extending from the plasma membrane to the dense midline. The ODP is characterized by two distinct dense regions: an approximately 4 nm thick region located approximately 10 nm from the plasma membrane and an approximately 8 nm thick electron-dense region located approximately 20 nm from the plasma membrane (Fig. 1*C*). The locations of these regions overlap with the peaks of the distribution of the gold labels in the immuno-EM studies on desmosomes and correspond to the positions of the N- and C-termini of the plakophilin and plakoglobin, respectively (11). The immuno-EM studies also show that, in addition to plakophilin and plakoglobin, the ODP contains the cytoplasmic domains of the desmosomal cadherins and the N-terminal region of desmoplakin. For simplicity, we refer to the approximately 8 nm thick layer as the "plakoglobin layer" and the approximately 4 nm thick layer as the "plakophilin layer." The higher number of proteins in the plakoglobin layer is evident from its higher density (i.e., low intensity) compared with the plakophilin layer (Fig. 1*C*). Furthermore, the plakoglobin layer has the same density as the dense midline. Because the intensity of the recorded images is linearly dependent on the density of the protein complexes, we can closely estimate the stoichiometries of the constituent components. Hence, given the size of the first extracellular domain (EC1) of the cadherins involved in the interaction at the dense midline, and the sizes of plakophilin, desmoplakin, and plakoglobin, we conclude that the plakoglobin layer contains the same amount of protein complexes as the dense midline. The plakophilin layer contains half the number of complexes compared with the dense midline, and therefore the same number of complexes as the number of cadherins emanating from the cell surface.

The plakoglobin and plakophilin layers indicate a quasi-periodicity of approximately 7 nm, as seen in the autocorrelation function, which can be followed over several molecules and is very similar to the quasiperiodicity of the extracellular region

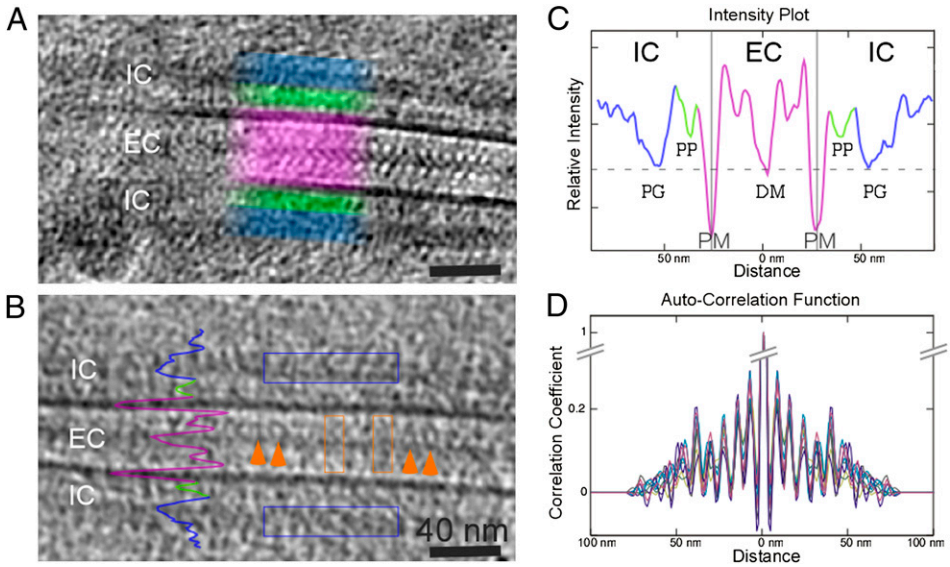

Fig. 1. Ultrastructure of the desmosome from human epidermis. (*A*) Two-dimensional projection image of a straight desmosome shows the periodic structure in extracellular and intracellular regions. The extracellular desmosomal cadherins appear as electron-dense protrusions extending from the plasma membrane (PM) to a dense midline (DM), showing a pronounced periodicity (purple boxed area). At the intracellular region (IC), two layers with different levels of intensity (green and blue highlighted area) can be observed, corresponding to the plakophilin and plakoglobin layers. (*B*) A 6-nm-thick tomographic slice shows details of the desmosomal interactions in extracellular and intracellular spaces. *cis* interactions (cadherin emanating from the same cell) are highlighted by the orange arrows; *trans* interactions (cadherins emanating from juxtaposed cells), with the characteristic "W" shape, are boxed in the orange areas. The density profile of *C* is indicated on the image. (*C*) Graph of relative density as projected orthogonally to the normal of the plasma membrane (in three different colors corresponding to the different regions of the desmosome). The plasma membranes have the highest density, followed by the plakoglobin (PG) layer with a similar density to the dense midline, and finally the plakophilin (PP) layer with the lowest density. The comparable densities between the plakoglobin layer and the dense midline indicate a similar number of proteins clustering at these regions. (*D*) Superimposed autocorrelation function calculated at various positions of the desmosomal plaque (indicated with blue box in *B*) shows that the plaque has a periodicity of approximately 7 nm, which matches that of the extracellular region. (Scale bars: *A* and *B*, 40 nm.)

(Fig. 1*D*). We focused our analysis on the ODP regions because, when we processed the IDP, we could not obtain any significant densities or periodic patterns. We recorded several tomograms at different defocus settings ranging from −4 to −8 μm. The resulting 3D reconstructions were consistent with each other and showed similar periodicity, which enabled us to independently confirm the molecular architecture (Fig. S1 and Table S1).

Desmosomal Plaque Is an Ordered Array. To improve the signal, we rotationally aligned subtomograms (which were selected around the highest density positions of the plakophilin layer) according to their autocorrelation properties, with subsequent translational alignment (16). To analyze the structure of the plaque, we generated a number of individual subtomograms from several desmosomal regions. After subtomogram averaging and classification, the resulting map had a resolution of approximately 3.2 nm (according to the 0.5 criterion of the Fourier shell correlation; Fig. S2). The densities in the plakophilin layer are approximately 4 nm long and approximately 3 nm thick and produce a quasi-2D crystal layer arranged parallel to the plasma membrane. Their dimensions fit well to the structure of the arm repeats of the plakophilin (17). The unit cell has a parallelogram arrangement with side lengths of 7.5 nm and 6.8 nm and an angle of approximately 80° (Fig. S3), which is similar to the cadherin arrangement of the extracellular space (16). The area between plakophilin and plakoglobin appears smooth, indicating flexible regions that have been smoothed out after subtomogram averaging. In contrast to the N-terminal of plakoglobin, the N-terminal domain of plakophilin, consisting of 250 aa, is predicted to be largely unstructured and is likely to span this area. Furthermore, the plakophilins are shifted compared with the plakoglobin layer, and are accessible from the cytoplasmic side without interference from complexes within the plakoglobin layer. The plakophilins do not have obvious contacts with the membrane or with the densities observed in the plakoglobin layer. Although it is not visible, this does not exclude interactions between the two layers, as it is well known from many in vitro studies that N-terminal domain of plakophilin interacts mainly with N-terminal desmoplakin and cytoplasmic domains of desmosomal cadherins.

The densities in the plakoglobin layer form a stacked repeating zigzag pattern (Fig. 2*C*), with the molecules tilted with respect to the plasma membrane. At favorable views, the shape of the plakoglobins can be recognized (Fig. 2*D*). A number of studies using freeze-fracture and EM of chemically fixed and stained samples reported 5- to 8-nm-wide "traversing filaments" perpendicular to the plasma membrane and suggested that these filaments are associated with the IFs spanning the whole plaque and even penetrate the plasma membrane and interact with the extracellular domains in both desmosomes and hemidesmosomes (18–20). Because of the limited resolution of our map, the densities corresponding to the arm repeats of plakophilin and plakoglobin, the desmoplakin N terminus and the cytoplasmic domains of desmosomal cadherins cannot be individually distinguished. However, the complex structure built from these components is clearly visible.

Modeling of the Plaque Components. To gain insights into the interactions between the desmosomal components, we modeled the plaque components from the available structures or structural homologues (*SI Materials and Methods*). The arm repeats of plakophilin and plakoglobin, and part of the cytoplasmic domains of E-cadherins, have been crystallized alone or in complex (17, 21). The structures of the cytoplasmic domains of desmoglein (Dsg) and desmocollin (Dsc) are not available. However, an alignment of their sequences with those of E-cadherin shows that most of the observed E-cadherin/β-catenin interactions are likely to be conserved in desmosomal cadherin/plakoglobin complexes (22). Therefore, we modeled plakoglobin-binding residues of desmosomal cadherins on the E-cadherin/β-catenin structure (22). Most of the cytoplasmic domain of Dscs (approximately 150 among approximately 200 aa) is modeled based on the E-cadherin/β-catenin structure. The cytoplasmic region of Dsg is significantly larger and cannot be accounted for in our model. We speculate that the remaining region of the cytoplasmic domains of Dsg could span the region between the ODP and IDP, as proposed from sequence analysis (23), and thus it is not shown in our map of the ODP. The residues closer to the membrane interact with the unstructured N terminus of the plakophilin and have been averaged out. However, in individual images, the connections are clearly visible. The N terminus of desmoplakin interacts with most of the ODP components. The N terminus consists of 1,056 aa, and based on analysis of sequence conservation, it was predicted to consist of two pairs of spectrin repeats interrupted by a putative Src homology 3 (SH3) domain (24). It has been shown that the plakin

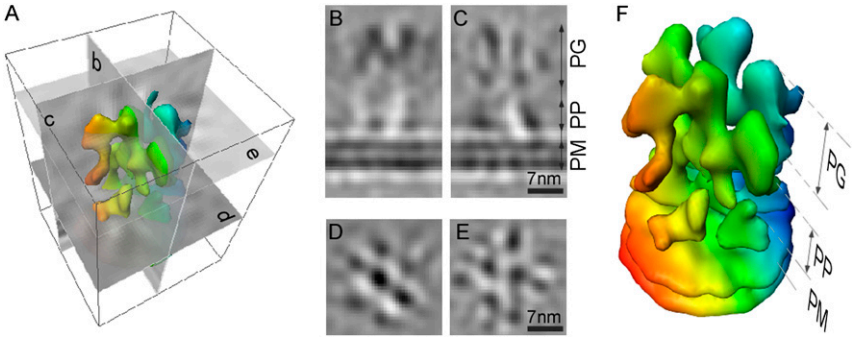

Fig. 2. Three-dimensional average of desmosomal plaque. (*A*) Illustration shows isosurface of the 3D average (350 subtomograms) of the intracellular part of the desmosome and the computational sections along the three axes visualized in *B*–*E*. (*B*) Coronal slice (0.6 nm thick) through the subtomogram average (as indicated by the letters in the illustration) show that the molecules in the plakoglobin layer form a zigzag pattern. The plakoglobin layer does not have obvious connections to the plakophilin layer. The area between the two regions appears smooth, electron-lucent, and unstructured. (*C*) Sagittal slice (0.6 nm thick) through the subtomogram average. The cross-sections of two molecules are shown, showing a remarkable similarity to the cross-sections of plakoglobin molecules. (*D* and *E*) Two 0.6-nm-thick axial slices through the plakophilin and the plakoglobin layers, respectively (*E* and *F*). A clear periodicity can be observed in both layers. Superposition of the two layers shows that the molecules in the plakophilin layer are shifted with respect to the plakoglobin layer, and are hence accessible from the cytoplasmic side. (*E*) Interconnections between the various molecules are visible. (Scale bars: 7 nm.) (*B*) The isosurface of the subtomogram average shows three distinct density layers, colored in three different colors: the plasma membrane (PM) and the plakophilin (PP) and plakoglobin layers (PG). The threshold is chosen so that the thickness of the central densities corresponding to the plakoglobin molecules is approximately 3.5 nm. The color coding varies as a function of the depth from red to blue. Individual layers are labeled with similar color. The interacting molecules form a zigzag pattern and are arranged in consecutive layers.

domain, consisting of the first 584 aa of the desmoplakin, interacts with plakophilin and plakoglobin. Furthermore, the colocalization of this plakin domain and of endogenous desmoplakin (DP) at cell–cell contacts, suggests that sequences necessary and sufficient to direct the association of DP with desmosomal plaque components during desmosome assembly are contained within the plakin domain. Importantly, the clustering of desmosomal cadherins and plakoglobin was observed only in the presence of the DP-NTP (N-terminal polypeptide containing the first 584 residues) (6). This domain alone could explain the density of the ODP as it was shown in DP-NTP–containing junctional structures that ultrastructurally exhibit ODPs closely resembling the plaque in normal desmosomal junctions (25). Based on these observations, we suggest that the remaining desmoplakin N terminus is localized further away from the ODP and is therefore not modeled. This plakin domain is a common feature of all plakin molecules including desmoplakin. Recently, a stable fragment of BPAG1, a major plakin protein localized to the hemidesmosomes, has been crystallized (24). The structure consists of two pairs of spectrin repeats, which share approximately 35% sequence identity with the plakin region of desmoplakin. Interestingly, this structure has significant structural similarity to α-catenin, the plaque protein of adherens junctions, despite the lack of significant sequence homology. β-Catenin mediates the interactions between α-catenin and E-cadherins, similar to the way in which plakoglobin mediates the interaction between desmoplakin and desmosomal cadherins. α-Catenin has been crystallized with the α-catenin binding helix of β-catenin [Protein Data Bank (PDB) ID code: 1dow]. Plakoglobin shares high sequence identity (>80%) with β-catenin. This high sequence identity is reflected by the substitution of plakoglobin by β-catenin in mouse tissues lacking plakoglobin (26). Given this high identity, we use the crystal structure of α-catenin/β-catenin (PDB ID code: 1dow) to fit into our EM density map. Although plakoglobin is common to both adherens junctions and desmosomes, α-catenin is excluded from desmosomes as a result of the overlap of binding sites of α-catenin and desmosomal cadherins, as has been shown by mutagenesis studies (7, 27). We suggest that this variation is a result of the subtle differences between desmoplakin and α-catenin in the binding sites in plakoglobin. This is supported by the observation that a few residues in the N terminus of the plakin domain can be highly divergent among members of the plakin family, including desmoplakin, which potentially contributes to the specificity of their biological functions (24). The residues at the tip of the desmoplakin N terminus were shown to interact with the plakophilin N terminus. This region is largely unstructured and thus it is likely to have been averaged out in the map.

Fitting X-Ray Structures into the Density Map. The plakophilin layer consists of individual densities, the sizes of which match remarkably well to the size of the arm repeats of the plakophilin structure. The rotational placement is partially defined through the positions of the C- and N-termini, as determined from immuno-EM, and the underlying density, although the axial orientation of the molecules cannot be defined. The molecules are thus placed in the context of the densities as defined by five of the six degrees of freedom.

The fitting of the molecules in the plakoglobin layer is significantly more demanding, because our resolution does not allow for direct recognition of the plakoglobin and the N-terminal part of desmoplakin. Placing these molecules into the density map by conventional cross-correlation methods only is ambiguous, given the limited resolution of the subtomogram average. By using the available information from various sources, we made the following assumptions: the orientation of the plakoglobin can be roughly set by the immunogold labeling studies, i.e., the C- and N-termini of the plakoglobin molecules are located closer and further away from the plasma membrane, respectively; the structures of desmoplakin and plakoglobin behave as rigid bodies; desmoplakin and plakoglobin build a complex that is flexibly tethered and is similar to β-catenin/α-catenin, as they are structural homologues; and the density map with the distinct zigzag pattern sets the best constraint in which the resulting structures should fit comfortably. In the following, we apply similar algorithms as described by Alber et al. (28, 29), with the main difference being that our main underlying information for the fitting is the density map.

The first consideration for the fitting is the number of molecules involved in the plakoglobin layer. We set our artificial "unit cell" to include the equivalent of at least four cadherins, so the plakophilin layer has at least four molecules fitted. According to our density calculations, the plakoglobin layer should include either eight plakoglobin molecules with a stoichiometry of 2:1 (plakoglobin:Dsc) or four plakoglobin molecules and four desmoplakin molecules with a stoichiometry of 1:1 (plakoglobin:Dsc and desmoplakin:Dsc) (Fig. S6 *A* and *B*). In the first case, the desmoplakin molecules would be located outside the plakoglobin layer, and would be flexibly tethered to it, so that they smooth out during the averaging process, as no additional densities were obtained there. For the application of the genetic algorithms (GAs), we started with various configurations and various stoichiometries, with the three most prominent configurations presented in Fig. S4.

The outcome of the GA shows an arrangement of plakoglobin/desmoplakin positioned at an angle of approximately 40° with respect to one another. Thus, the desmoplakin has to be bent approximately 100° compared with the arrangement of α/β-catenin suggested in Huber and Weis (22), which results in a good fit to the density map without any visible clashes (Fig. 3). This hinge flexibility can be associated with the presence of proline residues in the helical regions of β-catenin, which are rotated in the E-cadherin and XTcf-3 complexes.

Many sequences of Dsg and Dsc corresponding to sequences of E-cadherins observed in E-cadherin/β-catenin interactions are conserved in plakoglobin/desmosomal cadherin complexes. Furthermore, the corresponding residues of desmosomal cadherins at the hinge position have been suggested to be particularly important in plakoglobin/desmosomal cadherin interactions (22). We suggest that these residues might influence the rotation of the helical regions of plakoglobin, resulting in more flexible motion of the hinge.

Our fitting results in three distinct configurations with very similar merit figures, and they outperform any other configuration (also with other stoichiometries) (Fig. S5 and Fig. S6). In the most favorable configuration, plakoglobin and desmoplakin molecules are arranged in alternating patterns (Fig. S6 *E* and *F*). In the configuration with alternating homophilic dimers of plakoglobin and desmoplakin (Fig. S6 *C* and *D*), we could not find any evidence of dimerization of plakoglobin. Even more significantly, it has been explicitly reported that the N-terminal part of α-catenin (the homologue of desmoplakin) does not dimerize when bound to β-catenin (30). Our configuration (Fig. 3) satisfies a number of pieces of biochemical evidence. Desmosomal cadherins are in a 1:1 stoichiometry with plakoglobin (21, 31). Our fitting implies a stoichiometry of desmoplakin and plakoglobin of 1:1. Furthermore, our fitting shows a second potential binding site of desmoplakin on the central arm repeats of plakoglobin. The multiple binding sites of desmoplakin on plakoglobin demonstrate unique properties of plakoglobin in recruiting desmoplakin to desmosomes, as it has been shown by mutagenesis studies (6). This function was shown in plakoglobin-KO keratinocytes, in which the cytoplasmic plaque appeared sparse and anchoring of IFs was defective (10, 26). Although the β-catenin was shown to substitute for plakoglobin in clustering desmosomal cadherins, which appeared intact in the extracellular region showing a dense midline, it was unable to recruit normal levels of desmoplakin to the plaque; this was man-

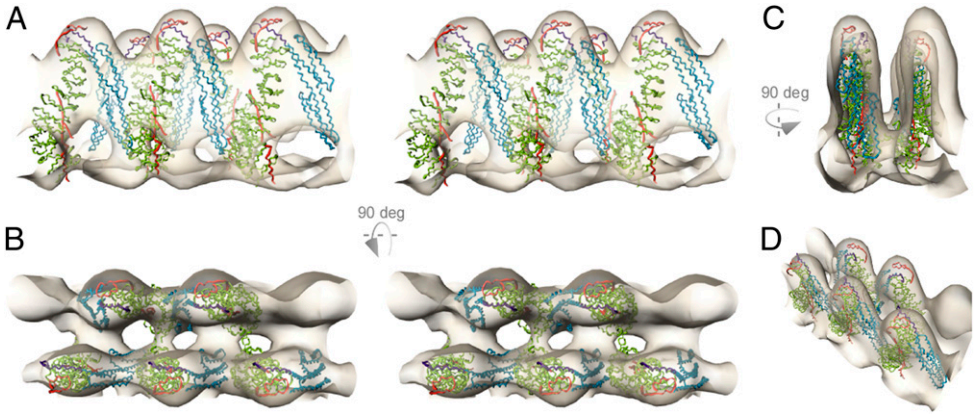

Fig. 3. Fitting of plakoglobin X-ray structures onto the symmetrized plakoglobin layer. (*A*) Crossed-eye stereo representation of the isosurface of the symmetrized subtomogram average of the plakoglobin layer (in beige) on which the X-ray structures of an alternating plakoglobin/desmoplakin (green/blue) complex has been placed. The cytoplasmic region of the cadherins is indicated in red. Five individual plakoglobin/desmoplakin complexes were accommodated into the density map. The zigzag structure of the plakoglobin layer is clearly visible. The desmoplakin molecules connect to the plakoglobin molecules at two positions: on the upper part close to the N terminus and in the central armadillo repeats. (*B*) The same representation as in *A* rotated 90°. Next to the zigzag structure shown in *A*, an additional connection between plakoglobins or other densities can be observed, indicating lateral connections in two directions. (*C*) The same representation as in *A* rotated 90° around a different axis. This is the typical view observed on 2D EM images. (*D*) Arbitrary perspective view of the same structure.

ifested in a substantially less dense and thinner ODP, and the IDP was devoid of IFs in these cells.

In contrast to previous EM studies, our resulting configuration provides direct verification of in situ stoichiometry of the plaque proteins, which partially verifies in vitro binding studies as well as revealing information about the stoichiometry. However, because of the limited resolution of our density map and imprecision of the positions determined by the immunogold labeling, we are unable to unambiguously assign the observed densities to individual plaque components. The reasons for this are twofold: (*i*) the available structures are relatively small to be fitted into cryo-ET images, and (*ii*) the available structures look very similar at the resolution obtained by electron tomographic studies. By integrating the information from immuno-EM, biochemical, and mutagenesis studies, our resulting configuration is the best possible explanation of the complex structure of the desmosomal plaque in situ. Our density map might be better explained if a significantly higher resolution map could be produced (with a resolution at approximately 1.5 nm), or if the interacting components were solved as complexes.

Desmosomal Assembly. Our resulting 3D density map of the plaque and our previous density map of the extracellular space explain, at molecular resolution, the interdependence of the ordered structures observed intra- and extracellularly. This interdependence and matching of the order is illustrated in Fig. 4. The depiction clarifies the structural roles of the arm repeats of plakoglobin in interactions with both Dsg and Dsc; and the role of plakophilin, which interacts with desmosomal cadherins and desmoplakin through its N terminus (7, 27, 31, 32). Our results indicate that the arrangement of the extracellular domains we previously observed depends on an ordered structure within the plaque. Interestingly, the clustering of desmosomal cadherins and plakoglobin was observed only when the plakin domain of the desmoplakin was present (6). This order is important for maintaining tissue integrity. It has been shown that perturbation by phosphorylation of plaque components causes loss of order within the extracellular space and consequent loss or weakening of desmosomal adhesiveness associated with human genetic or autoimmune disease and wounds, respectively (33, 34). The observed matching of the periodic arrangement of both extracellular cadherins and the plaque supports these studies. The ordered structure of the plaque observed in our density map, as well as in regions in the vicinity of the desmosome, implies a sequential model of desmosomal assembly. We propose that the plakoglobin molecules provide a template on which the desmosomal cadherins cluster at the cell surface. Subsequently, *cis*- and *trans*-adhesive interactions are initiated between the extracellular domains of the cadherins. More and more cadherin/plakoglobin complexes are added to reinforce the newly formed junction. The plaque proteins desmoplakin and plakophilin are then added to the cadherin/plakoglobin scaffold as a molecular reinforcement to the junction by tethering to the IFs via the desmoplakin C terminus. Similar to the extracellular region of desmosome, the strong connection of the desmosomes to the cytoskeleton results from a cooperative mechanism in which a large number of molecules of the desmosomal plaque interact in a specific manner, resulting in a highly organized structure. Our density map suggests that the strong physical adhesion of desmosomes arises from molecular clustering of the plaque components forming both lateral and medial molecular connections.

Conclusions

The organization of the cytoplasmic plaque of intercellular junctions such as desmosomes and adherens junctions, as well as

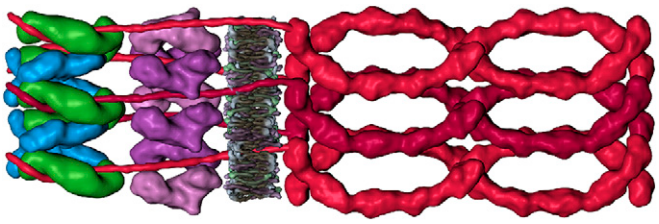

Fig. 4. The complete desmosome structure. The drawing combines the complete knowledge of the interactions of the various desmosomal components on the basis of the cryo-ET data. The interactions of both plaque components and the extracellular cadherins (16) are visualized in the map. Two molecular layers representing five to six unit cells in the extracellular and intracellular parts are shown. The plakoglobin molecules are depicted in green, the desmoplakin in light blue, plakophilins in purple, and the desmosomal cadherins (Dsg and Dsc) in two shades of red. The periodicity of the extracellular layer matches the periodicity of the plaque components remarkably well, suggesting that they are connected by their flexible cytoplasmic tails to the plakoglobin molecules.

ECM-cell focal adhesions and hemidesmosomes has been controversial; the major challenge is the molecular crowdedness. Although immunogold EM, biochemical, and mutagenesis studies have provided important information on the positions and interactions between the constituent proteins, the molecular architecture of how these proteins interact and are organized in the context of assembled junctions was missing. Our approach by using cryo-ET of vitreous sections combined with 3D averaging provides the arrangement of the proteins in situ and in vivo. In combination with constrained fitting, which integrates information from other techniques, the most probable 3D arrangement of the molecular players is presented. However, the resolution does not allow for the unambiguous identification of the constituent proteins. For this to be achieved, a twofold resolution improvement is necessary, given the similarity of the complexes involved; or alternatively, high-resolution structures with larger domains, ideally with more than one of the interacting molecules cocrystallized, are required. Our approach with cryo-ET of vitreous sections combined with 3D averaging is currently the only technique that has the potential to visualize the structural organization of the cytoplasmic surface of major intercellular junctions in normal and diseased tissue.

Materials and Methods

Human skin biopsy specimens 150 μm in size and 100 μm in thickness embedded in 1-hexadecence, immediately after extraction, were cryofixed in an EMPACT2 high-pressure freezer (Leica Microsystems). Cryosections of nominal thickness of 50 nm were generated in an EM FC6/UC6 ultramicrotome (Leica Microsystems) at −140 °C and at a cutting speed of 1.0 mm/s by using a 35° diamond knife (Diatome). The cryosections were collected in CFlat 4/2 200 or 300 mesh carbon copper grids (Electron Microscopy Science) and attached using a electrostatic charging device (Leica Microsystems). The cryosections were then labeled with PbS quantum dots of approximately 10 nm (Evident Technologies) according to the protocol of Masich et al. (35). Single-axis tilt series of desmosomal regions in the epidermis covering an angular range from −65° to +65° with 1° or 2° angular increment were recorded in a Tecnai G2 Polara microscope (FEI) that had been cooled to liquid nitrogen temperature and equipped with a postcolumn GIF 2002 energy filter (Gatan). The tilt series were recorded under low-dose conditions by using the UCSF tomography software (36). Images were recorded on a 2,000 × 2,000 pixel CCD camera at a defocus level between −9 and −4 μm (pixel sizes are 1 nm and 0.6 nm at the specimen level; Table S1). The total electron dose was approximately 4,000 e^-/nm^2 per tilt series. The projection images of the tilt series were aligned using the quantum dots. The merit figure of the aligned series used for the reconstruction and subsequent processing had a value of less than 0.6 nm, which indicates proper alignment and suggests that the section did not deform during the acquisition. We performed the reconstructions by using weighted back-projection algorithms and visualized them with isosurface- and volume-rendering techniques in the Amira software package (Mercury Computer Systems). Sequence similarity detection by HHM was used to model plakoglobin binding residues of Dsg based on the structure of epithelial cadherin (PDB ID code: 1i7w), plakophilin based on the solved human plakophilin structure (PDB ID code: 1xm9), and the desmoplakin/plakoglobin complex using structure of the complex α-catenin/β-catenin (PDB ID code: 1dow).

ACKNOWLEDGMENTS. We thank W. Kuehlbrandt, B. Boettcher, and J. Dubochet for suggestions and critically reading the manuscript. We thank Zhou Yu for help with Fig. 4. This work was supported by FP6 Marie Curie mobility network grants and EMBO fellowships (to A.A.-A.), the FP6 3D repertoire network of excellence (R.B.R.), and an ERC Starting Grant (to A.S.F.).

1. McKoy G, et al. (2000) Identification of a deletion in plakoglobin in arrhythmogenic right ventricular cardiomyopathy with palmoplantar keratoderma and woolly hair (Naxos disease). *Lancet* 355:2119–2124.
2. McGrath JA, et al. (1997) Mutations in the plakophilin 1 gene result in ectodermal dysplasia/skin fragility syndrome. *Nat Genet* 17:240–244.
3. Bornslaeger EA, et al. (2001) Plakophilin 1 interferes with plakoglobin binding to desmoplakin, yet together with plakoglobin promotes clustering of desmosomal plaque complexes at cell-cell borders. *J Cell Sci* 114:727–738.
4. Chen X, Bonne S, Hatzfeld M, van Roy F, Green KJ (2002) Protein binding and functional characterization of plakophilin 2. Evidence for its diverse roles in desmosomes and beta -catenin signaling. *J Biol Chem* 277:10512–10522.
5. Kapprell HP, Owaribe K, Franke WW (1988) Identification of a basic protein of Mr 75,000 as an accessory desmosomal plaque protein in stratified and complex epithelia. *J Cell Biol* 106:1679–1691.
6. Kowalczyk AP, et al. (1997) The amino-terminal domain of desmoplakin binds to plakoglobin and clusters desmosomal cadherin-plakoglobin complexes. *J Cell Biol* 139: 773–784.
7. Troyanovsky RB, Chitaev NA, Troyanovsky SM (1996) Cadherin binding sites of plakoglobin: Localization, specificity and role in targeting to adhering junctions. *J Cell Sci* 109:3069–3078.
8. Smith EA, Fuchs E (1998) Defining the interactions between intermediate filaments and desmosomes. *J Cell Biol* 141:1229–1241.
9. He W, Cowin P, Stokes DL (2003) Untangling desmosomal knots with electron tomography. *Science* 302:109–113.
10. Acehan D, et al. (2008) Plakoglobin is required for effective intermediate filament anchorage to desmosomes. *J Invest Dermatol* 128:2665–2675.
11. North AJ, et al. (1999) Molecular map of the desmosomal plaque. *J Cell Sci* 112: 4325–4336.
12. Al-Amoudi A, et al. (2004) Cryo-electron microscopy of vitreous sections. *EMBO J* 23: 3583–3588.
13. Al-Amoudi A, Studer D, Dubochet J (2005) Cutting artefacts and cutting process in vitreous sections for cryo-electron microscopy. *J Struct Biol* 150:109–121.
14. Pierson J, Ziese U, Sani M, Peters PJ (2010) Exploring vitreous cryo-section-induced compression at the macromolecular level using electron cryo-tomography; 80S yeast ribosomes appear unaffected. *J Struct Biol* 173:345–349.
15. Pierson J, et al. (2010) Improving the technique of vitreous cryo-sectioning for cryo-electron tomography: Electrostatic charging for section attachment and implementation of an anti-contamination glove box. *J Struct Biol* 169:219–225.
16. Al-Amoudi A, Díez DC, Betts MJ, Frangakis AS (2007) The molecular architecture of cadherins in native epidermal desmosomes. *Nature* 450:832–837.
17. Choi HJ, Weis WI (2005) Structure of the armadillo repeat domain of plakophilin 1. *J Mol Biol* 346:367–376.
18. Kelly DE, Kuda AM (1981) Traversing filaments in desmosomal and hemidesmosomal attachments: Freeze-fracture approaches toward their characterization. *Anat Rec* 199:1–14.
19. McNutt NS, Weinstein RS (1973) Membrane ultrastructure at mammalian intercellular junctions. *Prog Biophys Mol Biol* 26:45–101.
20. Miller K, Mattey D, Measures H, Hopkins C, Garrod D (1987) Localisation of the protein and glycoprotein components of bovine nasal epithelial desmosomes by immunoelectron microscopy. *EMBO J* 6:885–889.
21. Choi HJ, Gross JC, Pokutta S, Weis WI (2009) Interactions of plakoglobin and beta-catenin with desmosomal cadherins: basis of selective exclusion of alpha- and beta-catenin from desmosomes. *J Biol Chem* 284:31776–31788.
22. Huber AH, Weis WI (2001) The structure of the beta-catenin/E-cadherin complex and the molecular basis of diverse ligand recognition by beta-catenin. *Cell* 105:391–402.
23. Nilles LA, et al. (1991) Structural analysis and expression of human desmoglein: A cadherin-like component of the desmosome. *J Cell Sci* 99:809–821.
24. Jefferson JJ, Ciatto C, Shapiro L, Liem RK (2007) Structural analysis of the plakin domain of bullous pemphigoid antigen1 (BPAG1) suggests that plakins are members of the spectrin superfamily. *J Mol Biol* 366:244–257.
25. Bornslaeger EA, Corcoran CM, Stappenbeck TS, Green KJ (1996) Breaking the connection: displacement of the desmosomal plaque protein desmoplakin from cell-cell interfaces disrupts anchorage of intermediate filament bundles and alters intercellular junction assembly. *J Cell Biol* 134:985–1001.
26. Bierkamp C, Schwarz H, Huber O, Kemler R (1999) Desmosomal localization of beta-catenin in the skin of plakoglobin null-mutant mice. *Development* 126:371–381.
27. Witcher LL, et al. (1996) Desmosomal cadherin binding domains of plakoglobin. *J Biol Chem* 271:10904–10909.
28. Alber F, et al. (2007) Determining the architectures of macromolecular assemblies. *Nature* 450:683–694.
29. Alber F, et al. (2007) The molecular architecture of the nuclear pore complex. *Nature* 450:695–701.
30. Pokutta S, Weis WI (2000) Structure of the dimerization and beta-catenin-binding region of alpha-catenin. *Mol Cell* 5:533–543.
31. Chitaev NA, Averbakh AZ, Troyanovsky RB, Troyanovsky SM (1998) Molecular organization of the desmoglein-plakoglobin complex. *J Cell Sci* 111:1941–1949.
32. Wahl JK, et al. (1996) Plakoglobin domains that define its association with the desmosomal cadherins and the classical cadherins: Identification of unique and shared domains. *J Cell Sci* 109:1143–1154.
33. Amagai M (1995) Adhesion molecules. I: Keratinocyte-keratinocyte interactions; cadherins and pemphigus. *J Invest Dermatol* 104:146–152.
34. Sen-Chowdhry S, Lowe MD, Sporton SC, McKenna WJ (2004) Arrhythmogenic right ventricular cardiomyopathy: Clinical presentation, diagnosis, and management. *Am J Med* 117:685–695.
35. Masich S, Ostberg T, Norlén L, Shupliakov O, Daneholt B (2006) A procedure to deposit fiducial markers on vitreous cryo-sections for cellular tomography. *J Struct Biol* 156:461–468.
36. Zheng SQ, et al. (2007) UCSF tomography: An integrated software suite for real-time electron microscopic tomographic data collection, alignment, and reconstruction. *J Struct Biol* 157:138–147.